Available online at www.sciencedirect.com

jmr&t Journal of Materials Research and Technology

journal homepage: www.elsevier.com/locate/jmrt

Shear performance of reinforced expansive concrete beams utilizing aluminium waste

Yasin Onuralp Özkılıç [a,**], Memduh Karalar [b], Ceyhun Aksoylu [c], Alexey N. Beskopylny [d], Sergey A. Stel'makh [d], Evgenii M. Shcherban [d], Shaker Qaidi [e], Iully da S.A. Pereira [f], Sergio Neves Monteiro [g], Afonso R.G. Azevedo [h,*]

[a] Department of Civil Engineering, Necmettin Erbakan University, Konya 42000, Turkey
[b] Department of Civil Engineering, Zonguldak Bulent Ecevit University, Zonguldak, 67100, Turkey
[c] Department of Civil Engineering, Konya Technical University, Konya 42130, Turkey
[d] Don State Technical University, Rostov-on-Don, 344003, Russia
[e] Department of Civil Engineering, College of Engineering, University of Duhok, Duhok, 42001, Iraq
[f] UENF - State University of the Northern Rio de Janeiro, LAMAV - Advanced Materials Laboratory, Av. Alberto Lamego, 2000, Campos Dos Goytacazes, 28013-602, Brazil
[g] IME - Military Institute of Engineering, Department of Materials Science, Square General Tibúrcio, 80, Rio de Janeiro, 22290-270, Brazil
[h] UENF - State University of the Northern Rio de Janeiro, LECIV - Civil Engineering Laboratory, Av. Alberto Lamego, 2000, Campos Dos Goytacazes, 28013-602, Brazil

ARTICLE INFO

Article history:
Received 27 December 2022
Accepted 14 April 2023
Available online 21 April 2023

Keywords:
Reinforced concrete
Beam
Shear
Aluminum waste
Expansive
Concrete
Reused

ABSTRACT

Shear damage is a catastrophic failure in the design of reinforced concrete structural elements. To prevent it, the effect of aluminum wastes on reinforced concrete shear beams was investigated in this study. There is a gap in the scientific field on the expanding concrete with aluminium waste, and no research has been done on the utilizing of aluminum waste to produce expandable concrete. Moreover, there is a gap in expandable concrete usage with aluminum waste reinforcing, which is crucial for engineering applications especially beams, slabs and columns. For this purpose, experimental investigations were performed on a total of 12 Reinforced Concrete Beams (RCB) with different aluminum waste ratio (0, 1, 2 and 3 vol.%) and different shear reinforcement spacing (270, 200 and 160 mm). The depth span ratio was chosen as 1.6, 2.0 and 2.7. RCB was simply supported on the loading frame and subjected to four-points bending. As a result of experimental tests for each sample, the maximum load, stiffness, ductility and energy dissipation capacity were calculated. It was observed that the load capacity of the Al refuse combined RCBs raises as the vacancy of the stirrup reinforcement reductions compared with reference RCBs. Furthermore, it was found that the load capacity of the RCBs reduced as the Al refuse quantity in the concrete mixture was increased from 0% to 3%. However, it was found that the decrease in load capacity for 1 vol.% aluminum waste could be tolerated. For this reason, it can be stated that aluminum waste (AW) in reinforced concrete shear beams will contribute to the beam up to 1%.

* Corresponding author.
** Corresponding author.
E-mail addresses: yozkilic@erbakan.edu.tr (Y.O. Özkılıç), afonso@uenf.br (A.R.G. Azevedo).

https://doi.org/10.1016/j.jmrt.2023.04.120

1. Introduction

Urbanization, which has developed in parallel with the growth of the population, has continuously developed the technology of concrete, which is one of the primary building materials of the construction industry [1–3]. Indeed, fresh concrete can be easily brought into the desired shape due to its plastic state. It can be produced both on-site and prefabricated. It has a relatively high compressive strength in the hardened state, and its service life is long; labor costs for construction and repair works are less than many other materials. In addition, fresh concrete is more economical than other building materials [3]. However, the tensile strength of concrete remains very low. Dissimilar conventional materials with higher tensile strength were employed to as reinforcement raise the low tensile strength of concrete [4,5]. These materials, such as steel, polymeric or natural fibers, usually are used to improve the low tensile characteristics of concrete by using dissimilar types of refuse materials based on circular economy. Studies on increasing the dissimilar tensile specifications of concrete were constantly being put forward with dissimilar materials and methods. Mineral additives and pozzolans, as well as chemical additives, were employed to reduce the water/cement percentage (w/c), together with fiber reinforcement, and now are widely spread methods that increase concrete strength [6–13]. Kozak [14] stated that using steel fiber was an effective way to raise the fracture resistance and ductility of concrete against the static and dynamic loads. Yildiz et al. [15] concluded that while the tensile strength of glass fiber-reinforced concrete escalated, the ultrasonic sound permeability consequences were also reduced. Şimşek and Baharavar [16] stated that concrete workability decreases for dissimilar types of concrete as the amount of steel fiber raises. In addition, studies [16] examine the change in the tensile specifications of concrete by using refuse materials, such as fly ash.

The low tensile strength of the concrete was sometimes associated with fractures due to shrinkage and drying during the hardening process. Application of expansive concrete was one of the methods used to eliminate this disadvantage in concrete [17–21]. Expansive concrete can be attained using some expansion additives [22,23] that were based on cement minerals [18]. Expansion additives generally include iron powder, alumina powder, magnesia, calcium sulfate aluminate ($CaO–A1_20_3–SO_3$), and calcium oxide (CaO) [18].

When producing durable concrete, alumina-rich binders and chemical additives such as lithium salts can be used to prevent the expansion caused by the alkali–silica reaction (ASR) in concrete [24,25]. The role of aluminum (Al) in reducing ASR is related to decrease the dissolution rate of the reactive silica. In addition, the presence of Al can change the structure of crystalline ASR to produce zeolite or its precursor. This effect seems to be important under natural conditions of environment due to the slow kinetics of zeolite formation [24,26]. The presence of Al leads to a slower SiO_2 dissolution and, thus, a slower formation of reaction products [24]. The addition of Al causes a chemical reaction that produces hydrogen gas. The more gas develops, the mortar expands, and the air content in the concrete rises. As the Al percentage raises, the expansion rate and the final expansion amount raise [25,27].

On the other hand, the raise in Al causes an important decrease in concrete strength [27]. In addition, Al powder is also used as an air entrainment agent to prevent concrete expansion caused by the ASR reaction, which forms pores [28]. It is shown that with the raise of the Al powder content, the number of pores increases, and the expansion of the concrete decreases.

As aforementioned, refuse materials are widely employed today to change the tensile specifications of concrete [29,30]. Such materials, which have little economic value, can be utilized as a by-product and source of the reused product in dissimilar sectors. Along with these refuse materials, it was possible to reduce the environmental problems they might cause by open disposal [31–45]. In particular, non-degradable refuse materials can remain in the environment for thousands of years. One of these refuse materials was the Al waste obtained in Computer Numerical Control machining (CNC).

Since Al is a lighter, easily processed, and more corrosion-resistant material than steel, the use of Al is quite common in many sectors, and the amount of Al waste, either powder or particles of fibers, generated as a consequence of this situation is increasing [46,47]. Gödek et al. [48] investigated the usability of Al waste particles released by the CNC production technique instead of fiber in cement paste and designated that this can improve the inflection and energy absorption ability of brittle cement-based material. Sabapathy et al. [46] experimentally investigated the mechanical specifications of concrete by using dissimilar amounts of Al fibers in concrete and revealed that these fibers contribute significantly to concrete's tensile and compression strengths. Muwashee et al. [49] used Al waste as fiber in mortar and concrete, revealing that concrete's compressive, tensile, and inflection strengths escalated. Çabalar et al. [50] investigated the usability of spiral Al milling refuse in the pavement subbase. Kumar et al. [51] reported on the use of Al and steel scrap refuses in place of fine aggregate materials in dissimilar proportions in regard to cement mass, and it was revealed that the tensile specifications improved importantly. Alfeehan et al. [52] investigated the improvement of the structural productivity of unidirectional ribbed plate (RS) panels by dissimilar types of industrial refuses, especially Al waste, and stated that the strength of concrete escalated. Malek et al. [53] investigated the influence of the steel and Al chips coming out of the CNC benches on the specifications of the concrete and designated that the concrete density is reduced and the strength is escalated. Noori et al. [54] employed modified solid Al scrap to improve the specifications of cement mortar.

As a consequence of the extensive literature research, it was seen that the influence of Al wastes on Reinforced Concrete Beams (RCBs) with insufficient shear capacity was not investigated. Therefore, in this experimental study, Al CNC waste was added to RCBs at dissimilar proportion and tested

under vertical loads. In this way, change was surveyed, and it has been suggested that researchers should use Al CNC waste at certain proportion.

2. Materials and method

In this experimental investigation, aluminum wire was reused as a waste product from CNC machining. The employed waste of Al machine turnings are presented in Fig. 1. Average length of the Al wires was ranged 10–20 mm. The folds were formed when waste Al cables were passed through the machine for recycling. Using waste Al wires longer than 40 mm was prevented to avoid aggregation. For concrete manufacture, traditional Portland Cement (OPC) CEM I 32.5 R was consumed. The w/c percentage was 0.6. The cement aggregate percentage was 0.22. To obtain expanding concrete, different amounts of aluminum wire were used.

The beams with a length of 1 m were studied. Twelve RCB specimens were cast and tested at Necmettin Erbakan University. All specimens had 2φ6 compression reinforcement and 2φ12 tensile reinforcement, resulting in a reinforcement percentage of 0.0125. Stirrup spacings were selected to observe shear damage. Three different spacing of 27, 20 and 16 cm were selected. These intervals were preferred to observe the shear effect for beams.

On the other hand, three dissimilar fiber volume (V_f) percentages of 1%, 2% and 3% were selected. The specifications of the examples are presented in Table 1. The reinforcement details, expansion of concrete during the production stage, and test setup are illustrated in Figs. 2–4, respectively.

3. Experimental results and discussion

The effect of the different number of stirrups and Al wires on the rupture and bending behaviour of RCBs has been investigated and utilized. For this purpose, the pre-formed beams were tested for rupture and bending. As indicated above, a total of 12 tests were made for this purpose. After 12 different beams were arranged in the lab, these beams were exposed to four-point loading. These tests in the RCBs were assessed comprehensively, and it was confirmed that each AI quantity had a dissimilar rupture and bending consequences.

Fig. 1 – The reused aluminium wires employed in this experimental study.

Table 1 – Specimen coding and characteristics.

No	Name	Stirrups	V_f
1	S-REF1	Φ6/27	0%
2	S-REF2	Φ6/20	0%
3	S-REF3	Φ6/16	0%
4	S–CNC1	Φ6/27	1%
5	S– CNC 2	Φ6/20	1%
6	S– CNC 3	Φ6/16	1%
7	S– CNC 4	Φ6/27	2%
8	S– CNC 5	Φ6/20	2%
9	S– CNC 6	Φ6/16	2%
10	S– CNC 7	Φ6/27	3%
11	S– CNC 8	Φ6/20	3%
12	S– CNC 9	Φ6/16	3%

Additionally, dissimilar bending consequences were studied for each RCBs with different Al waste quantities. Each RCB shown divergent load-carrying capabilities, which was remarkable regarding the impact of Al waste amounts on the rupture and flexural behavior of concrete structures. For this experimental research, 12 dissimilar RCBs specimens were confirmed, as presented in Table 1.

3.1. *Impact of tension reinforcement on AW*

This section is devoted to the influence of the different number of stirrups on the rupture and shear behavior of RCBs that was assessed in detail as noted below.

3.1.1. *Condition 1: rupture and load–displacement of RCB (S-REF1, S-REF2, S-REF3)*

As attained by experimental consequences, it was surveyed important shear fractures in the RCB specimens depending on the vertical load. When perpendicular load was applying, the max deflections in the RCBs were recorded and shear fractures were obviously seen in this element as presented in Fig. 5. It was shown in Fig. 5 that the fractures can be surveyed in RCBs under large forces and noteworthy shear fractures were offered in Fig. 6.

These places of fractures were apparently associated with the place where vertical fractures can take place in the RCB. Furthermore, the max margin among the perpendicular fractures was found as 10.35 mm in the S-REF3 specimen (Fig. 5). As stated by Fig. 5, it was surveyed that the max shear fractures start from the place at the bottom where load was applied to the RCB, and these fractures extend up to the height of the beam. To obtain the numerical relations between bending deflection and perpendicular loads in RCB, the servo controlled hydraulic recorded both the mid-span deflection and loading RCB during the experimental tests. As presented in Fig. 6, load–displacement diagram was obtained for experimental beams. In regard to Fig. 6, it was investigated that bending of RCBs was associated with an almost straight

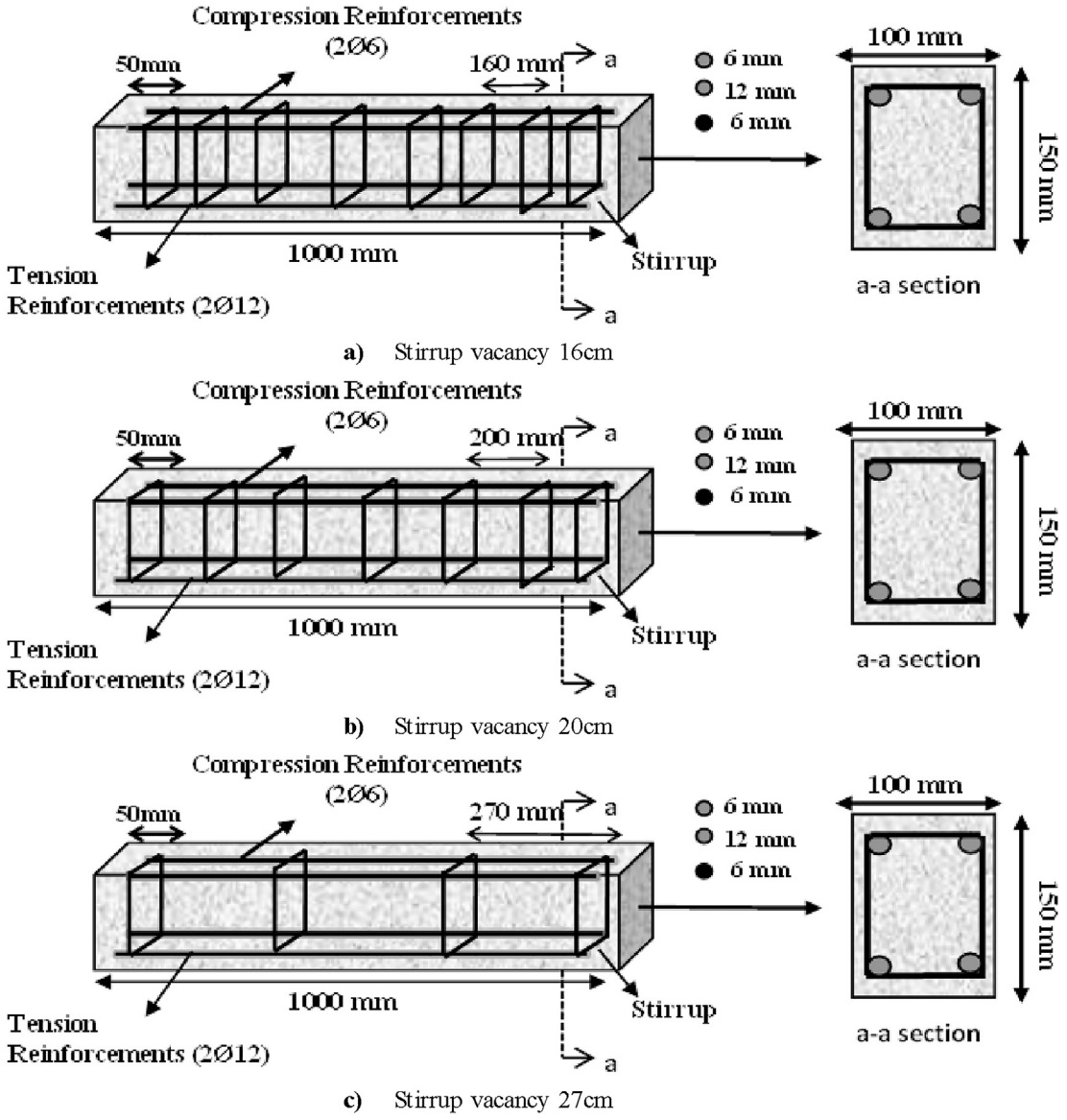

Fig. 2 – The general view of the reinforcement layout; a) stirrup spacing of 16 cm, b) stirrup spacing of 20 cm, c) stirrup spacing of 27 cm.

line until an ultimate point which relates to 33.44 kN, 45.35 kN and 58.71 kN for S-REF1, S-REF2, S-REF3, respectively. At that point, it was found that 3.27 cm, 7.66 cm and 6.37 cm bending deformation was surveyed for the max perpendicular load for S-REF1, S-REF2, S-REF3. Subsequently, as the load reduced, the bending deformation was importantly increased. At the end of the experimental test, it was found that 3.39 cm, 14.29 cm and 10.36 cm max bending deformations obtained for S-REF1, S-REF2, S-REF3. The RCBs and RCB reduced their load at this bending value. These were noteworthy data about the load of the RCBs for S-REF1, S-REF2, S-REF3. For RCB specimens, when the stirrup spacing reduced from 270 to 200 mm and then to 160 mm, the bearing capacity of the RCBs increased. However, all three specimens failed because of shear rupture." Since the influence of stirrup spacing on the load bearing capacities of RCBs was observed, as estimated, while the stirrup spacing reduces, the load bearing abilities of the RCBs progressively rise as a result of the later occurrence of shear cracks in the RCBs. The influence of both concrete compressive strength and stirrup spacing on the ductility of RCBs was obviously realized in the load displacement diagrams. While the concrete compressive strength reduces, the rate of covering the principal tensile stresses in the RCBs by stirrups rises. While the stresses on the stirrups rise, the stirrups begin to yield. Consequently, as the concrete compressive strength reduced, the RCBs demonstrated a more ductile rupture.

3.1.2. *Condition 2: rupture and load–displacement of RCB (S–CNC1, S–CNC2, S–CNC3)*

As indicated by the experimental test consequences for S–CNC1, S–CNC2, S–CNC3, it was found remarkable shear fractures in the RCB depending on the perpendicular force. As

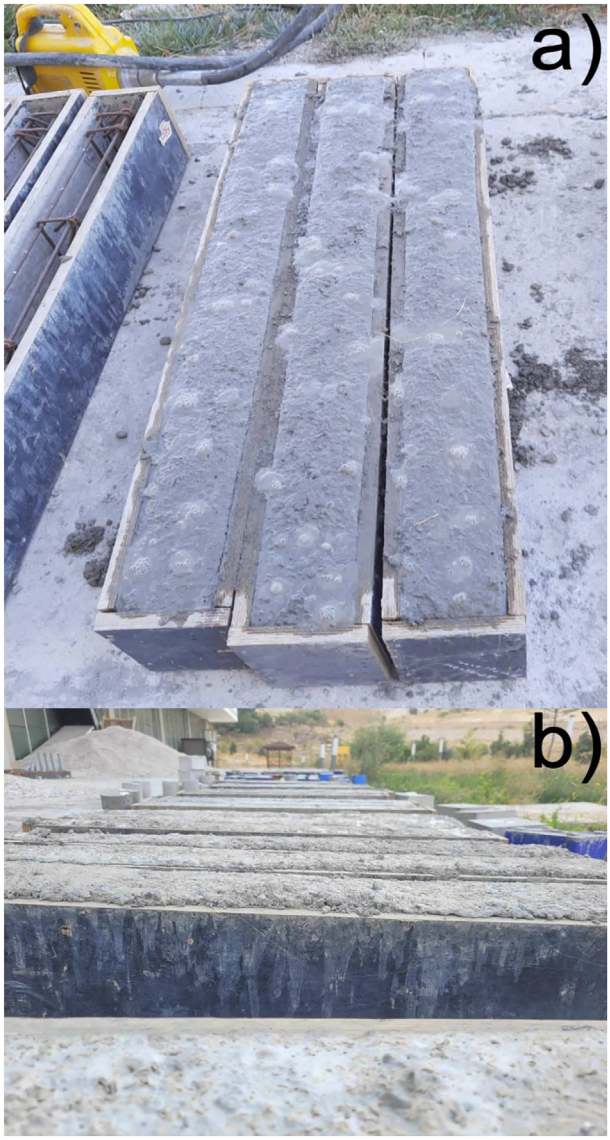

Fig. 3 – Expansion of concrete a) before setting, b) after setting.

surveyed in Fig. 7, shear fractures in the RCB were not evident under the perpendicular forces. Regarding to Fig. 7, it was of great importance that shear fractures were detected in the RCBs. The cracking of the RCBs was occurring between the point where the load was applied and the support region due to the diagonal load, which was presented in Fig. 7. This crushing was critical because it reveals the effect of the protecting behavior of stirrups and reinforcements on the bending behavior of RCBs. As also presented in Fig. 7, it was surveyed that important shear fractures were formed close to the support areas. These shear fractures were considerably vital to assess the fracture behavior of RCBs with dissimilar amount of stirrups. In other words, as the spacing of the stirrups in the RCB reduced (270 mm > 200 mm > 160 mm), the Al waste scraps had less influence on the bearing capacity of the RCB. This occurs at a steady Al refuse values of approximately 1% and related to the shear stresses covered by the stirrup was higher owing to the decrease in the stirrup spacing. As surveyed in Fig. 8, deformations recorded by LVTD were very important to evaluation the load–displacement behavior of RCB with dissimilar amount of stirrups. In accordance with Fig. 8, bending load follows an almost linearly until an ultimate point of this straight line achieves 31.69 kN, 42.89 kN and 52.57 kN for S–CNC1, S–CNC2, S–CNC3, respectively. At that point, it was found that 3.23, 7.41 and 6.91 mm bending deformations were surveyed at max vertical load for S–CNC1, S–CNC2, S–CNC3. Subsequently, though the load reduced, the bending was importantly greater than before. As presented in Fig. 8, it was surveyed that 7.40, 13.72 and 12.58 mm max. Bending deformations for S–CNC1, S–CNC2, S–CNC3, respectively, were observed at the end of the experimental test and RCB lost its load capacity at this bending values. These consequences disclosed the influence of dissimilar amount of stirrups on the bending-load behavior of the RCB. While testing RCBs with dissimilar amount of stirrups, important shear fractures and bending variations have been surveyed under the vertical load. Additionally, a smaller amount of bending deformation has been surveyed in the S–CNC3 because of frequent stirrup range, as compared with S–CNC1, S–CNC2.

3.1.3. *Condition 3: rupture and load–displacement behavior of RCB (S–CNC4, S–CNC5, S–CNC6)*

As presented by experimental test consequences for S–CNC4, S–CNC5, S–CNC6, there were important shear fractures in the beams relying on the perpendicular load. As offered in Fig. 9, the bending in the beams were surveyed under perpendicular loads. In regard to Fig. 9, it was noticeably that noteworthy shear fractures were detected in the RCB. In other words, as the stirrup spacing increased, shear rupture became more pronounced. In regard to Fig. 10, bending increased as an almost straight line until an ultimate point of this line, which were related to 26.84 kN, 41.64 kN and 48.49 kN for S–CNC4, S–CNC5, S–CNC6. At that point, it was surveyed that 2.21, 7.40 and 6.63 mm bending deformations were detected at max vertical load for S–CNC4, S–CNC5, S–CNC6. Subsequently, as the load was reduced, the bending deformation was importantly increased. As presented in Fig. 10, it was surveyed that 9.49, 8.36 and 10.68 mm max bending deformations for S–CNC4, S–CNC5, S–CNC6 were detected at the end of the test and the beams lost its load at corresponding bending values. These consequences clearly reveal the importance of data about the bearing ability of the RCBs (S–CNC4, S–CNC5, S–CNC6) with regard to stirrup spacing and percentage of Al waste.

3.1.4. *Condition 4: rupture and load–displacement behavior of RCB (S–CNC7, S–CNC8, S–CNC9)*

As surveyed by experimental test consequences for S–CNC7, S–CNC8, S–CNC9, there were significant shear fractures in the beams relying on the perpendicular load as offered in the Fig. 11. The cracking of the beams were taking place in the shear zone relying on the perpendicular load was confirmed in the Fig. 11. In regard to Fig. 12, flexural deformation increased as an almost straight line until an ultimate point related to 15.93 kN, 38.56 kN and 44.02 kN for S–CNC7, S–CNC8, S–CNC9, respectively. At that point, 1.70, 6.53 and 8.95 mm bending deformations were surveyed for max. Vertical load

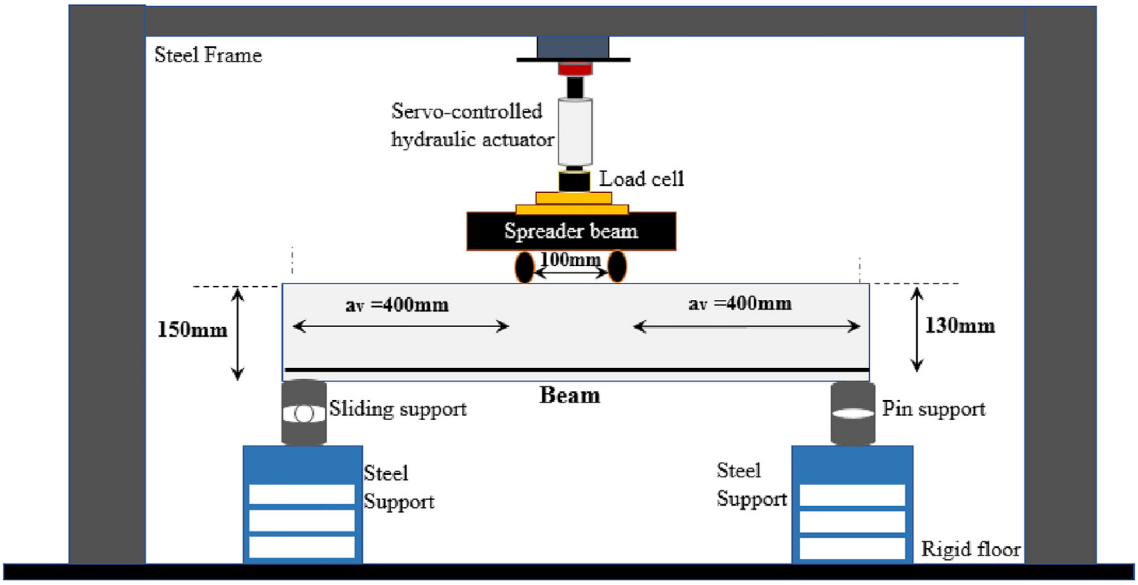

Fig. 4 – Experimental test setup.

for S–CNC7, S–CNC8, S–CNC9. Subsequently, as the load reduced, the flexural displacement was importantly greater than before. Test consequences detected that 11.33, 14.17 and 18.53 mm max. Bending deformations for S–CNC7, S–CNC8, S–CNC9 were surveyed at the end of test as a consequence, the beam lost its bearing capacity at this bending values. In these test consequences, it was found that the effect of dissimilar amount of stirrups influences the flexural behavior of the RCB.

Consequently, as can be surveyed from Figs. 6, 8, 10 and 12, the reference RCBs attained the max load capability in all stirrup spacing. Nonetheless, the bending ability of RCBs containing aluminum waste was decreased as the use of this waste was increased. In RCB specimens with stirrup spacing of 160, 200 and 270 mm, 0%, 1%, 2%, and 3% Al waste additives reduced the loading capacity of the RCBs compared to the reference RCB specimen. As it can be seen from these data given above, the amount of reduction in the loading forces changed depending on the stirrup gaps. As the spacing of the stirrups in the RCB was reduced from 270 to 200 mm and then to 160 mm, the Al waste had also a negative influence on the bearing capacity of the RCB at increasing Al waste values from

Fig. 5 – Fracture and shear behavior of RCB for S-REF1, S-REF2, S-REF3.

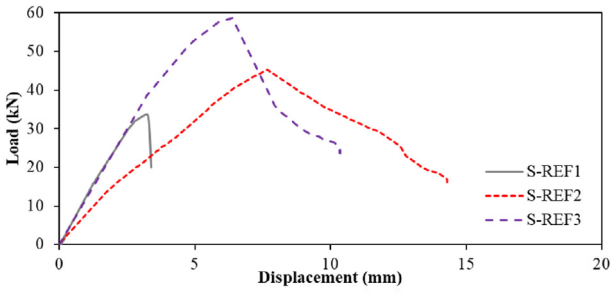

Fig. 6 – Load-deformation behavior of RCB for S-REF1, S-REF2, S-REF3.

0% to 3%. The reason for this, might be attributed to the share of shear stresses covered by the stirrup irons which was higher due to the decrease in the stirrup spacing. In the earlier studies, it has been observed that aluminum metal reacts with water (in alkaline solution of cement paste) and then produces aluminum hydroxide and hydrogen gas. Nonetheless, it has been argued that not all of this hydrogen gas was trapped in the mixture, but some of the gas comes out of the mixture at an early age and leaves the system [48]. This gas weakens the mixture because it creates air spaces in the concrete mixture. For this reason, it has been seen in studies that AW concrete causes a decrease in compressive strength, modulus of fracture and modulus of elasticity. Furthermore, as stated above, while the influence of stirrup spacing on the load bearing facilities of RCBs was associated with the stirrup spacing falls, the load bearing facilities of the RCBs progressively suffers an enlargement as a consequence of the later occurrence of shear fractures in the RCBs.

3.2. *Impact of Al waste ratio*

This section is devoted to the research of the influence of rates of Al waste on the rupture and shear behavior of RCBs was investigated fully. For this purpose, different amounts of Al waste were employed as 0%, 1%, 2% and 3% while the stirrups in the RCB was chosen as constant. Detail information was given as noted below.

3.2.1. *Condition 1: rupture and load–displacement behavior of proportion of AW for Φ6/27 stirrups*

The influence of dissimilar proportions of Al waste on the rupture and bending behavior of RCBs was actually considered. For this purpose, dissimilar amounts of AW were employed as 0%, 1%, 2% and 3% while stirrups in the RCB was chosen constant as Φ6/27. As presented by experimental test consequences for S-REF1, S–CNC1, S–CNC4 and S–CNC7, it was found that there were important shear fractures in the beams relying on the perpendicular load as depicted in Fig. 13. In regard to Fig. 14, bending deformations increased as an almost straight line until an ultimate point related to 33.44 kN, 31.69 kN, 26.84 kN and 15.93 kN for S-REF1, S–CNC1, S–CNC4 and S–CNC7, respectively. As presented in Fig. 14, it was found at that value of 3.27, 3.23, 2.21 and 1.70 mm for bending deformations were attained at max. Vertical load for S-REF1, S–CNC1, S–CNC4 and S–CNC7. Subsequently, as the load reduced, the bending deformation was importantly increased. Test consequences revealed that 3.39, 7.40, 9.49 and 11.33 mm were max. Bending deformations for S-REF1, S–CNC1, S–CNC4 and S–CNC7 found at the end of tests. Thus, the RCB lost its bearing capacity at these bending values. These

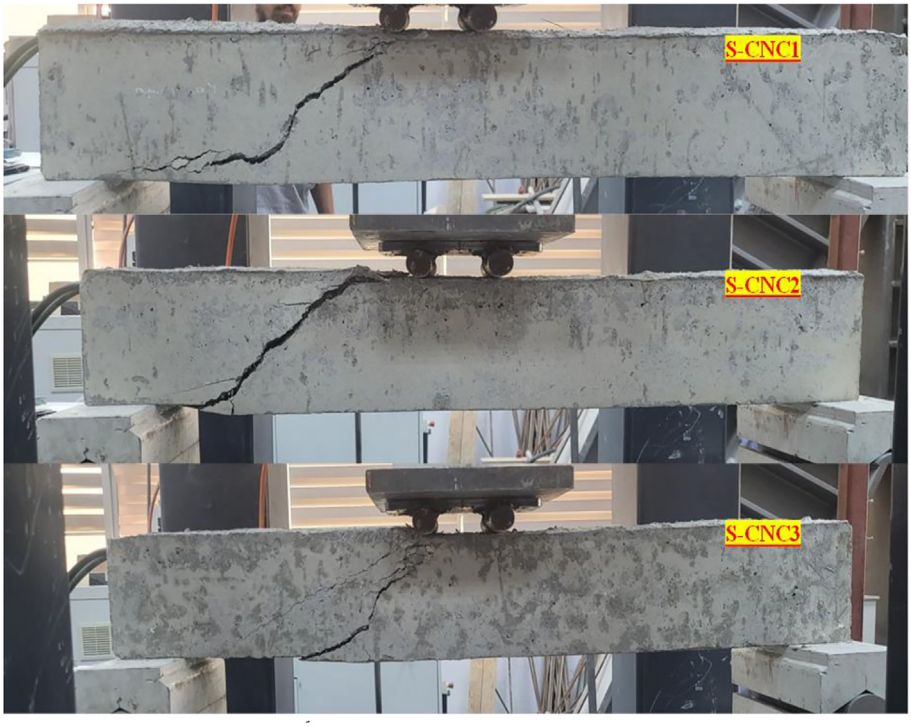

Fig. 7 – Fracture and shear behavior of RCB for S–CNC1, S– CNC2, S– CNC3.

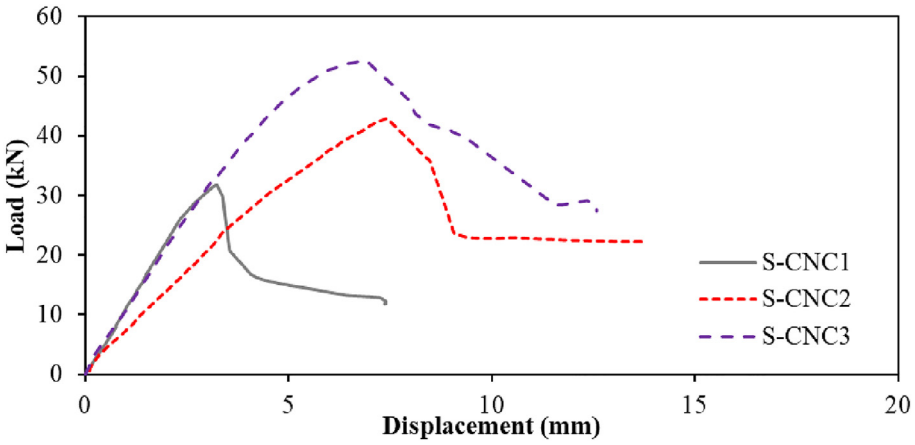

Fig. 8 – Load-deformation behavior of RCB for S–CNC1, S–CNC2, S– CNC3.

consequences disclosed unquestionably essential data about the load of the RCBs (S-REF1, S–CNC1, S–CNC4 and S–CNC7) for dissimilar amounts of Al waste. In other words, the specimen (S–CNC1) with 1% AW in beams with the same stirrup percentage showed almost similar behavior as the RCB reference specimen. Also, the raise in the amount of Al waste leads to a important decrease in the load.

3.2.2. *Condition 2: rupture and load–displacement behavior of proportion of AW for Φ6/20 stirrups*

In this section of the examination, while stirrups in the beams was kept constant as Φ6/20, amounts of Al waste were improved as 0%, 1%, 2% and 3% to examine the impact of dissimilar amounts of Al waste on the rupture and bending behavior of the beams. As attained by experimental test consequences for S-REF2, S–CNC2, S–CNC5 and S–CNC8, there were important shear fractures in the beams relying on the perpendicular load as depicted in Fig. 15. In regard to Fig. 16, the bending deformation increased as an almost straight line until an ultimate point of this straight line occurs related to 45.34 kN, 42.89 kN, 41.64 kN, and 38.56 kN for S-REF2, S–CNC2, S–CNC5 and S–CNC8, respectively. In Fig. 16, it was found at the end point that 7.66, 7.42, 7.40 and 6.53 mm bending deformations were detected for max. Vertical load for S-REF2, S–CNC2, S–CNC5 and S–CNC8. After the ultimate point, though the load was reduced, the bending deformation

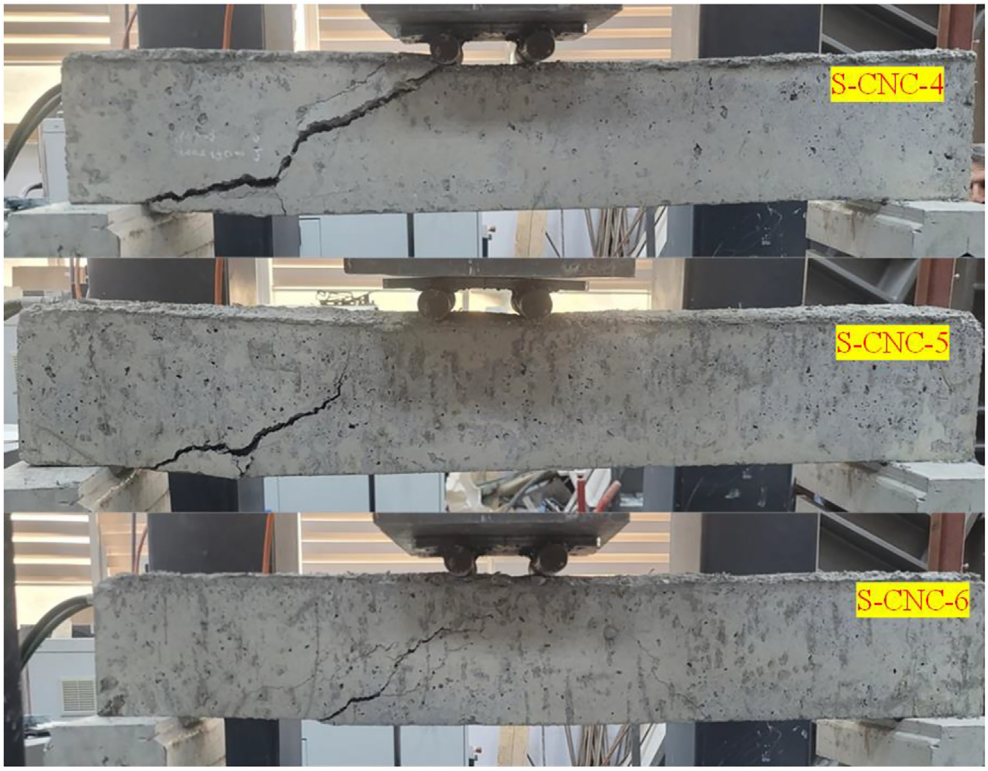

Fig. 9 – Fracture and shear behavior of RCB for S–CNC4, S–CNC5, S–CNC6.

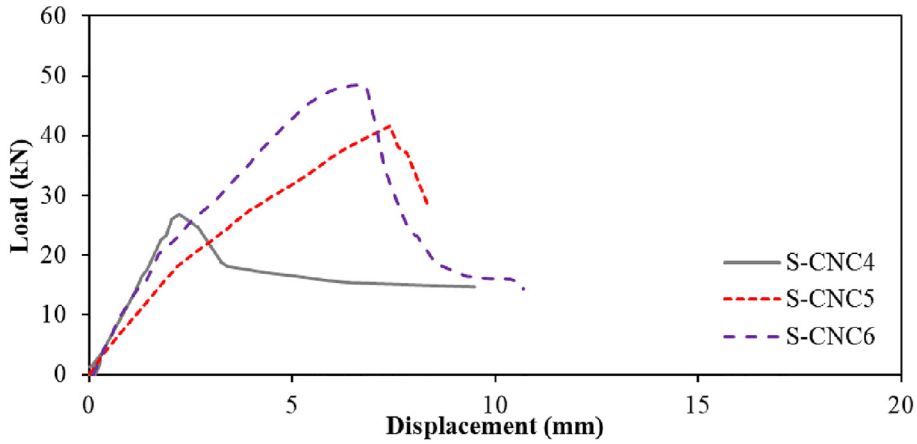

Fig. 10 – Load-deformation behavior of RCB for S–CNC4, S–CNC5, S–CNC6.

was extensively improved. While detecting the experimental test consequences, it was noticed that 14.29, 13.72, 8.36 and 14.16 mm max. Bending deformations for S-REF2, S–CNC2, S–CNC5 and S–CNC8 were surveyed at the end of corresponding tests. Consequently, the RCB lost its bearing capacity at this bending values. It's shown from the experimental test consequences, presented in Fig. 15, while amounts of Al waste were employed as 0% and 1%, it was detected that shear fractures occur in RCB. Furthermore, it was also found that important ruptures and bending alterations were surveyed for 0% and 1% under the perpendicular load in terms of RCB with dissimilar amounts of Al waste. Additionally, as detected from the experimental test consequences, it was observed that the load–displacement capacity of RCB reduces as the proportion of Al waste was increased for all quantities investigated.

3.2.3. *Condition 3: rupture and load–displacement behavior of proportion of AW for Φ6/16 stirrups*

In this part of the experimental study, while stirrups in the RCB were employed as a constant Φ6/16, proportions of Al waste were altered as 0%, 1%, 2% and 3% to observe the influence of these dissimilar amounts of waste on the rupture and bending behavior of RCBs. As surveyed by experimental test consequences for S-REF3, S–CNC3, S–CNC6 and S–CNC9, it was found that there were significant shear fractures in the beams relying on the perpendicular load as offered in Fig. 17. In regard to Fig. 18, the bending deformations improved as an almost straight line until an ultimate point was reached in this straight line related to 58.71 kN, 52.57 kN, 48.49 kN and 44.02 kN for S-REF3, S–CNC3, S–CNC6 and S–CNC9, respectively. At that ultimate point, 6.38, 6.91, 6.63 and 8.95 mm

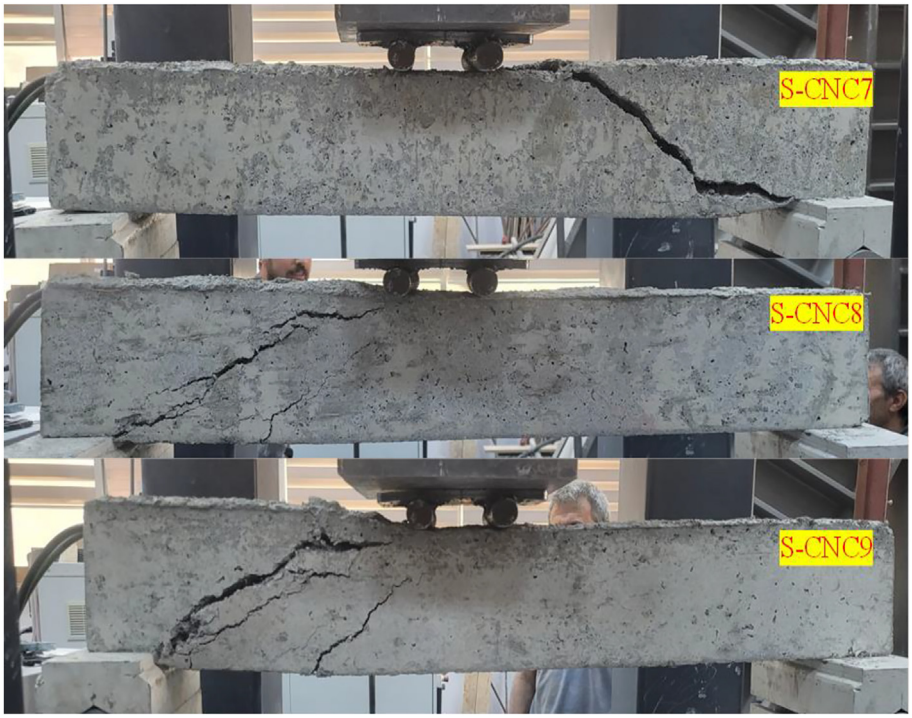

Fig. 11 – Fracture and shear behavior of RCB for S–CNC7, S–CNC8, S–CNC9.

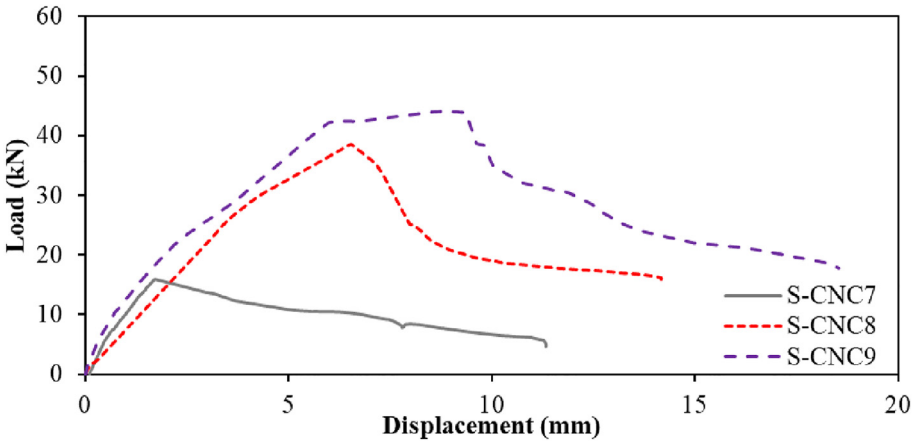

Fig. 12 – Load-deformation behavior of RCB for S–CNC7, S–CNC8, S–CNC9.

bending deformations were detected for the max. Vertical load for S-REF3, S–CNC3, S–CNC6 and S–CNC9. Subsequently, after the ultimate point, though the force was reduced, the bending deformation was significantly increased. During evaluation of the experimental test consequences, it was noticed that 10.36, 12.57, 10.69 and 18.53 mm were the max. Bending deformations for S-REF3, S–CNC3, S–CNC6 and S–CNC9 found at the end of the test. Moreover, the beams lost its load capacity at this final bending values. Additionally, it was noticed that dissimilar ruptures and bending changes were surveyed under the perpendicular force while comparing RCBs with dissimilar quantities of Al waste. Additionally, as revealed from the experimental test consequences, it was surveyed that the load–displacement ability of RCB increased as the quantity of Al waste increased for all investigated amounts. In Fig. 19, it might be realized that Al wires act as links among concrete parts.

As a consequence, it can be found from Figs. 14, 16 and 18 that the bearing capacity of the RCBs was reduced as the Al waste amount in the concrete combination was increased from 0% to 3%. As surveyed in the load-deflection curve, the deformation rises linearly with increasing loading. This was estimated since the stresses in the concrete and steel were comparatively lower and materials were in the elastic region of their mechanical behavior. In the elastic–plastic stage, there was an alteration in the slope of load-deflection curve. This was occurring because of cracking. Subsequently as cracking occurred, deformation raises again with load going

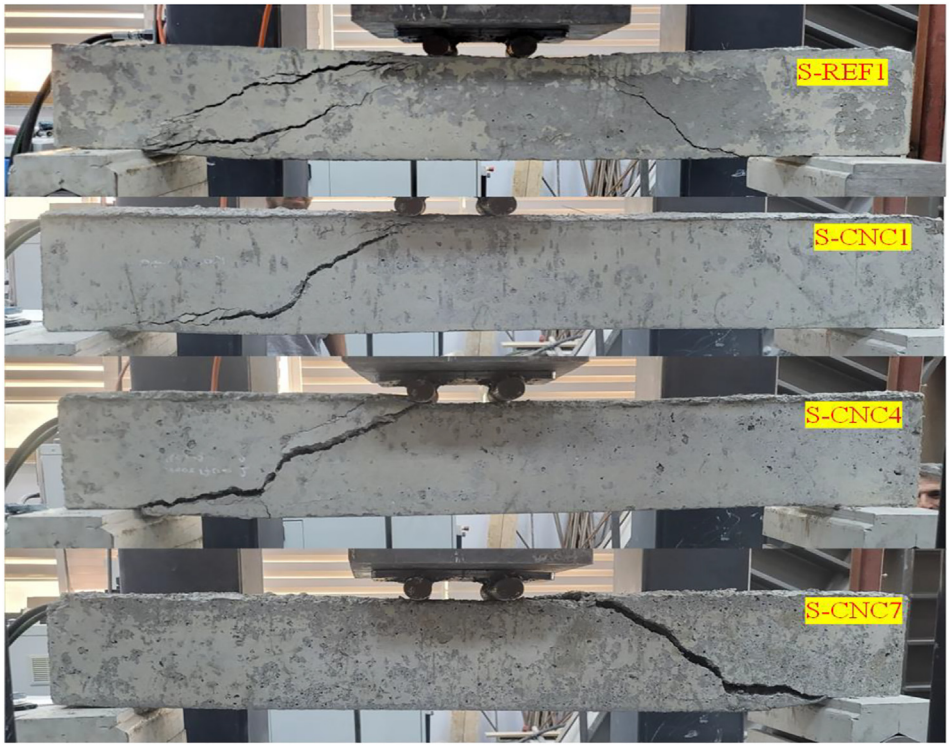

Fig. 13 – Fracture and shear behavior of RCB for S-REF1, S–CNC1, S–CNC4 and S–CNC7.

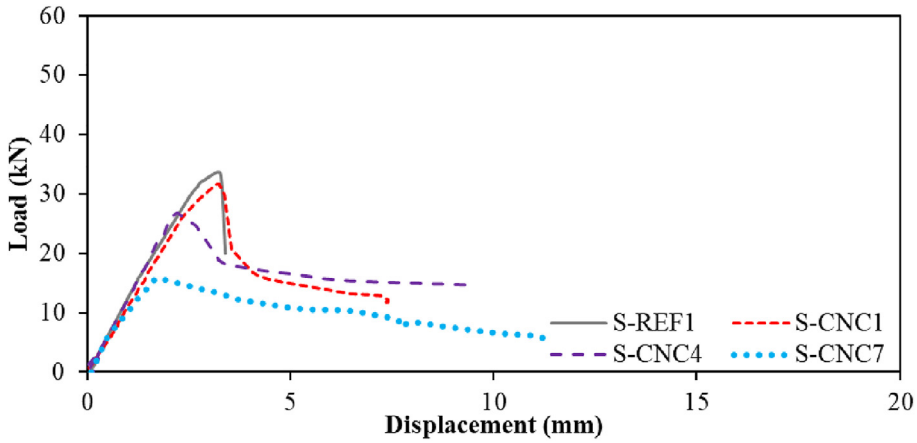

Fig. 14 – Load-Deformation behavior of RCB for S-REF1, S–CNC1, S–CNC4 and S–CNC7.

up to a point just before critical load in the reinforcement concrete beam. After that, there was no noticeable raise in the applied load until it reaches the fully plastic stage, and the deformation was surveyed to raise importantly. Compared to the reference concrete, it was surveyed that Al waste did not have a noteworthy consequence on the load deformation behavior in the pre-cracking stage. It was also realized that these consequences were similar to those reported in the literature [55]. After the first cracking occurred, Al wastes had a negative effect on the stiffness and deflection behavior of the beams due to the formation of air voids in the concrete combination [55]. While the greater proportion of Al wastes caused poorer stiffness and greater deformations at same applied load. Furthermore, it was surveyed that Al waste reduced the amount and range of the flexural fractures in reinforcement concrete beams. It was also seen that these consequences were similar to those reported in the literature [55].

Ductility is one of the well-known parameters to be considered in the design of bending members. The structural ductility ratio of beams is calculated by beam mid-span flexure in the performed experimental tests. The structural ductility ratio is described here as the ratio among the final flexure and the flexure at the yield point of the longitudinal steel reinforcement. Further, at this point, the final flexure is described as the flexure at maximum load. Yield was obtained by estimates from the LVDTs placed at both sides of the cross division, parallel to the rebars. Table 2 offers ductility ratios

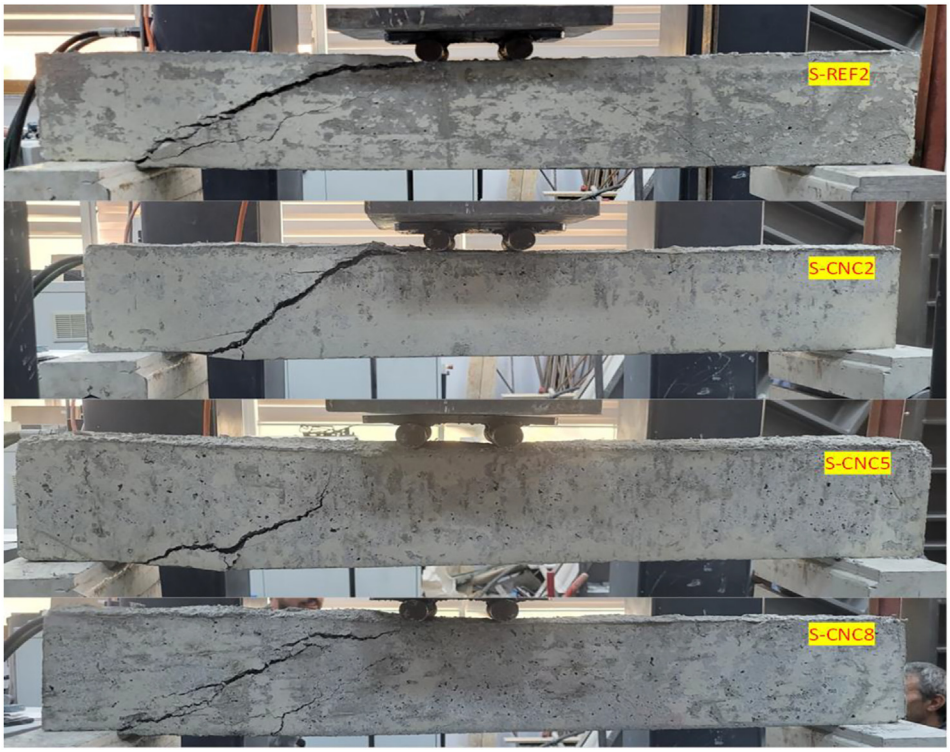

Fig. 15 – Fracture and shear behavior of RCB for S-REF2, S–CNC2, S–CNC5 and S–CNC8.

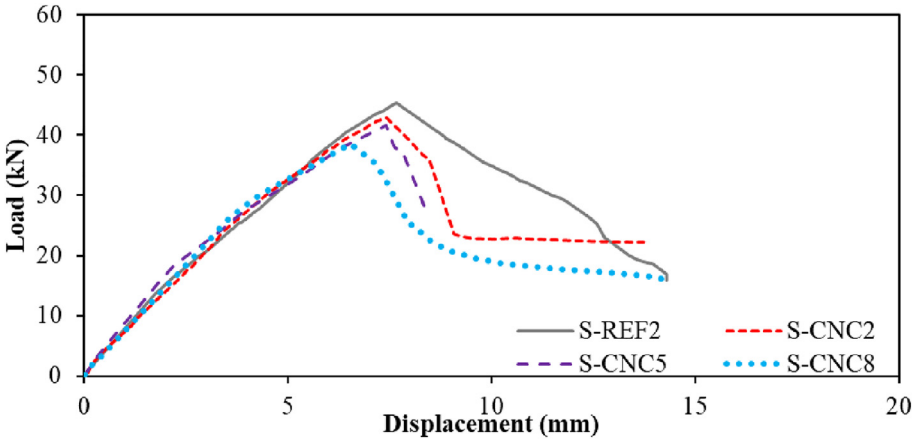

Fig. 16 – Load-deformation behavior of RCB for S-REF2, S–CNC2, S–CNC5 and S–CNC8.

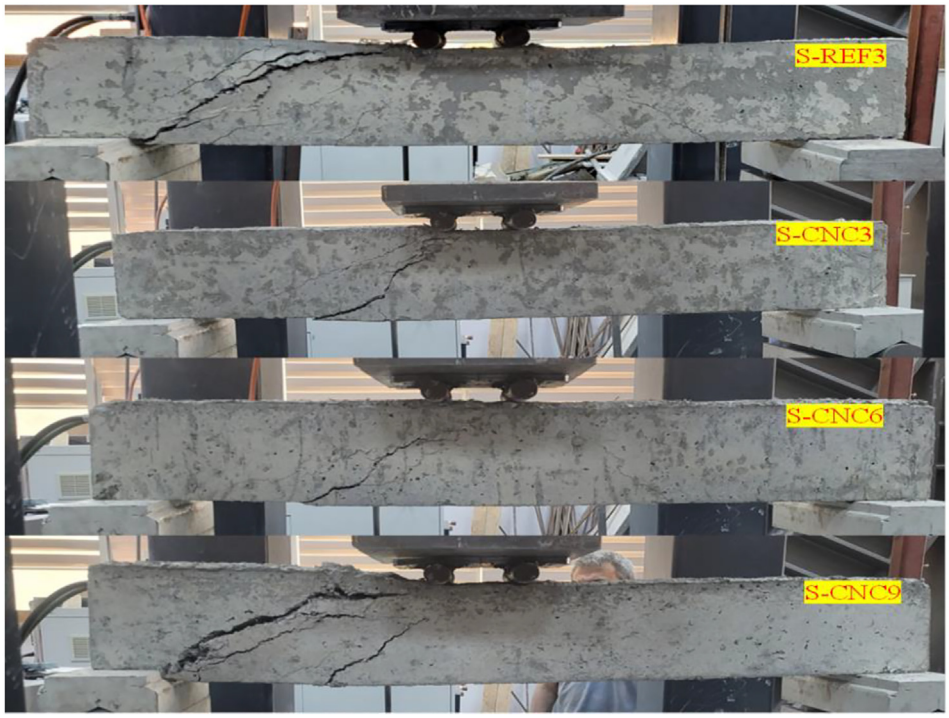

Fig. 17 – Fracture and shear behavior of RCB for S-REF3, S–CNC3, S–CNC6 and S–CNC9.

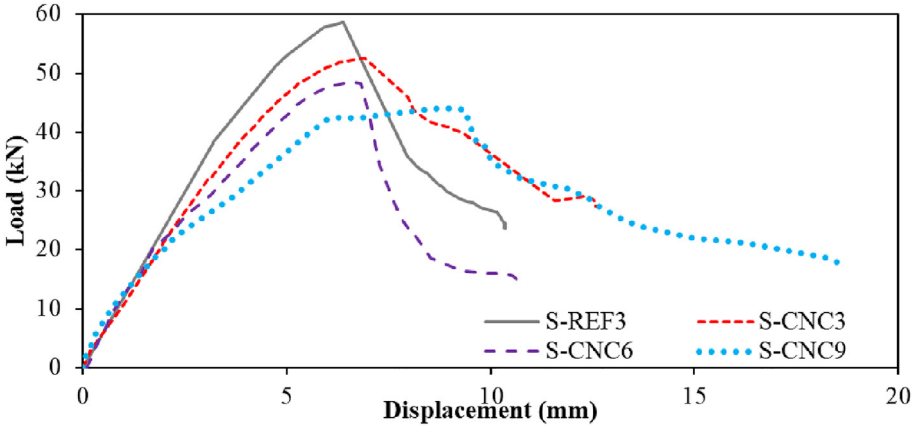

Fig. 18 – Load-deformation behavior of RCB for S-REF3, S–CNC3, S–CNC6 and S–CNC9.

Fig. 19 – Close view of specimen S–CNC3.

and ultimate flexures. As observed in Table 2, as the stirrup spacing decreases, the ductility ratio increases. Furthermore, the same trend is also observed in the 1% Al waste in the mixture. On the other hand, Energy dissipation is a coefficient that promote to the deformation procedure of a structural component. Energy dissipation can be defined as the ability of a structure to transmit energy during the reinforcement flow process. Therefore, it can be used to determine the damage mechanism of structures. Commonly, the damage mechanism is demonstrated as structural cracks or lack of reinforcement. Consequently, large dissipation energy is an perfect situation for structural components. While the energy dissipation is huge, plastic deformation can be achieved before failure take places. As can be observed in Table 3, energy dissipation capacities were given. As the stirrup spacing decreases, it was observed that the energy dissipation increases.

4. Shear calculation models

The shear resistance of RCBs can be designed in altered methods via empirical methods established on the expectations of the shear stress distribution theories in the beam element. Several shear calculation models are given in the literature. The correct estimation of test beam strength must be designed to take into account all of the various factors. These factors might be defined as cylinder strength, steel ratio, slenderness, web reinforcement stirrup ratio and stirrup yield stress. One of the most used in these Equations are given as following for altered concrete grades and based on altered

Table 2 – Experimental consequences for load and displacement values.

Test examples	P_{max} (kN)	Displ. at max Load (mm)	Rigidity (kN/mm) at (P_{max})	P_u ($0.85P_{max}$) (kN)	Displ. at yield δ_y (mm)	Rigidity (kN/mm) at yield ($0.85P_{max}$)	δ_u (mm)	Ductility ratio
S-REF1	33.44	3.27	10.21	28.42	2.40	11.81	3.31	1.37
S-REF2	45.34	7.66	5.92	38.54	6.06	6.35	9.12	1.50
S-REF3	58.71	6.37	9.20	49.90	4.56	10.93	6.98	1.53
S–CNC1	31.69	3.23	9.78	26.94	2.44	11.01	3.42	1.40
S– CNC 2	42.89	7.41	5.78	36.45	5.79	6.29	8.36	1.44
S– CNC 3	52.57	6.91	7.60	44.68	4.69	9.51	8.04	1.71
S– CNC 4	26.84	2.21	12.13	22.81	1.80	12.61	2.85	1.57
S– CNC 5	41.63	7.40	5.62	35.39	5.76	6.14	7.92	1.37
S– CNC 6	48.49	6.63	7.30	41.21	4.74	8.69	7.06	1.49
S– CNC 7	15.93	1.70	9.34	13.54	1.38	9.76	3.10	2.23
S– CNC 8	38.56	6.53	5.90	32.77	5.01	6.53	7.37	1.47
S– CNC 9	44.02	8.95	4.91	37.41	5.12	7.29	9.86	1.92

Table 3 – Experimental test consequences for energy dissipation capacities.

Test examples	Max. Dipsl. (mm)	Energy consumption at P_{max} (kj)	Energy consumption at $0.85P_{max}$ (kj)	Plastic energy consumption (kj)	Total energy consumption (kj)	Failure type	Ductility level
S-REF1	3.39	0.066	0.041	0.024	0.066	Shear	Deficient
S-REF2	14.29	0.243	0.138	0.260	0.399		
S-REF3	10.35	0.293	0.134	0.233	0.368		
S– CNC 1	7.39	0.061	0.053	0.069	0.122		
S– CNC 2	13.72	0.200	0.118	0.226	0.344		
S– CNC 3	12.57	0.276	0.139	0.299	0.438		
S– CNC 4	9.49	0.042	0.026	0.129	0.154		
S– CNC 5	8.36	0.190	0.128	0.088	0.215		
S– CNC 6	10.68	0.206	0.123	0.169	0.292		
S– CNC 7	11.33	0.033	0.011	0.100	0.111		
S– CNC 8	14.16	0.167	0.167	0.142	0.309		
S– CNC 9	18.53	0.276	0.148	0.383	0.531		

Table 4 – Comparing the equation with the test results.

Test examples	P_{max} (kN)	Zsutty, T. C. (1971).	Percent Change (%)
S-REF1	33.44	40.7	21.7
S-REF2	45.34	52	14.7
S-REF3	58.71	63	7.3
S–CNC1	31.69	37	16.8
S– CNC 2	42.89	47	9.6
S– CNC 3	52.57	57	8.4
S– CNC 4	26.84	33	23.0
S– CNC 5	41.63	43	3.3
S– CNC 6	48.49	52	7.2
S– CNC 7	15.93	32	100.9
S– CNC 8	38.56	40.9	6.1
S– CNC 9	44.02	49	11.3

shear transfer mechanisms. In the this model [56], available beam test data were divided into the distinct groups of altered strength behavior, and simple empirical calculations were derived for each group as offered in Eq. (1).

$$V_u = 2.1746\left(f_c'\rho\, d/a\right)^{1/3} b_w d + \frac{A_v f_y d}{s} \quad (1)$$

As observed in Table 4 is realized as the equation with the most approximate value. As can be understood from Table 4, it is detected that as the waste ratio in the mixture increases, the difference in change gradually increases.

5. Conclusions

In this experimental study, the shear and fracture behavior of various RCBs made from scrap aluminum was studied. For this purpose, three of these experimental specimens for testing were selected as reference specimens without any aluminum waste, while the others consisted of V_f of 1%, 2% and 3% of Al waste. During research, RCBs were arranged in the lab, and then these specific RCBs were subjected to bending tests using special devices. Then, the perpendicular load was applied to the RCBs with several Al waste amounts and bending in the RCBs was measured using servo controlled hydraulic recorded gadget. Fracture and shear performances of the RCBs were utilised in relation to the experimental and analytical tests in detail. These critical consequences were estimated as noted below.

- The influence of an altered amount of stirrups on the rupture and shear behavior of RCBs was observed in detail. At the end of the experimental test consequences, it was surveyed that the load capacity of the Al waste incorporated RCBs raises as the spacing of the stirrup reinforcement decreases compared with reference RCBs. On the other hand, when the influence of an amount of stirrups with Al waste on the rupture and shear behavior of RCBs were investigated, it was surveyed that the load capacity of the RCBs reduced as the Al waste amount in the concrete combination was increased from 0% to 3%.
- In regard to experimental test consequences, it might be pointed out that the maximum capacity of the beams reduces while the ratio of Al waste in the concrete combination rises. When RCBs with dissimilar Al waste quantities were compared, max. Bending occurred in the middle of the RCB was detected for S–CNC6 Al waste incorporated RCBs.
- It was confirmed that Al waste quantity considerably affects the fracture behavior of the RCBs. Important shear fractures were surveyed in the RCBs depending on the amount of Al waste. As the Al waste amount in the concrete combination was increased from 0% to 3%, it was noticed that the deformation capacity increased while the load capacity reduced.
- An approximation of 3%–23% was obtained between experimental and analytical studies. The waste ratio in the mixture increases, and the difference in change gradually increases.
- It was designated that the energy consumption capacity and total energy consumption capacity of the examples generally increased with the raise in the Al waste percentage.
- The reason for not obtaining positive influence on strength can be mainly attributed to two reasons:
  - o First, Al wastes were too short in terms of their lengths (approximately 10 mm). Previous studies revealed that medium lengths were optimum for adequate productivity on improvement in tensile forces [4,29].
  - o Second, the strength of Al waste was low to resist tensile fractures. The Al strength was importantly less when compared to that of steel lathe scraps. Previous studies [28] showed that steel lathe scraps have strength high enough to improve the flexural productivity of the beams.

This experimental research study revealed that Al waste can be employed to obtain expansive concrete. The optimum amount of 1% Al refuse can be consumed for this purpose. On the other hand, lower strength values were also noticed when higher amount of Al waste was employed. To address these shortcomings, future work will focus on using Al waste with a medium length.

Declaration of Competing Interest

The authors declare that they have no known competing financial interests or personal relationships that could have appeared to influence the work reported in this paper.

REFERENCES

[1] Panda SS, Senapati AK, Rao PS. Effect of particle size on properties of industrial and agro waste-reinforced aluminum-matrix composite. JOM 2021;73:2096–103.
[2] Bhoi NK, Singh H, Pratap S. Developments in the aluminum metal matrix composites reinforced by micro/nano particles–a review. J Compos Mater 2020;54:813–33.
[3] Roussel N, Bessaies-Bey H, Kawashima S, Marchon D, Vasilic K, Wolfs R. Recent advances on yield stress and elasticity of fresh cement-based materials. Cement Concr Res 2019;124:105798.

[4] Çelik Aİ, Özkılıç YO, Zeybek Ö, Özdöner N, Tayeh BA. Performance assessment of fiber-reinforced concrete produced with waste lathe fibers. Sustain 2022;14:11817.
[5] Zeybek Ö, Özkılıç YO, Çelik Aİ, Deifalla AF, Ahmad M, Sabri Sabri MM. Performance evaluation of fiber-reinforced concrete produced with steel fibers extracted from waste tire. Front Mater 2022;vol. 9.
[6] Hadzima-Nyarko M, Nyarko EK, Ademović N, Miličević I, Kalman Šipoš T. Modelling the influence of waste rubber on compressive strength of concrete by artificial neural networks. Materials 2019;12:561.
[7] Ilki A, Kumbasar N, Koc V. Low strength concrete members externally confined with FRP sheets. Struct Eng Mech 2004;18:167–94.
[8] Özkılıç YO, Aksoylu C, Arslan MH. Experimental and numerical investigations of steel fiber reinforced concrete dapped-end purlins. J Build Eng 2021;36:102119.
[9] Karaşin İB, Işık E. Impact on the building performance of subsequently cast concrete. Bitlis Eren Univ J Sci Technol 2017;7:7–11.
[10] Tayeh BA, Hadzima-Nyarko M, Zeyad AM, Al-Harazin SZ. Properties and durability of concrete with olive waste ash as a partial cement replacement. Adv Concr Constr 2021:11.
[11] Hadzima-Nyarko M, Nyarko EK, Lu H, Zhu S. Machine learning approaches for estimation of compressive strength of concrete. Eur Phys J Plus 2020;135:682.
[12] Agwa IS, Zeyad AM, Tayeh BA, Adesina A, de Azevedo AR, Amin M, et al. A comprehensive review on the use of sugarcane bagasse ash as a supplementary cementitious material to produce eco-friendly concretes. Mater Today Proc 2022;54:21–35.
[13] Singh S, Ramakrishna S, Gupta MK. Towards zero waste manufacturing: a multidisciplinary review. J Clean Prod 2017;168:1230–43.
[14] Kozak M. Çelik lifli betonlar ve kullanım alanlarının araştırılması. Teknik Bilimler Dergisi 2013;3:26–35.
[15] Yıldız S, Bölükbaş Y, Keleştemur O. Cam Elyaf Katkısının Betonun Basınç ve Çekme Dayanımı Üzerindeki Etkisi. Politeknik Dergisi 2010;13:239–43.
[16] Şimşek O, Baharavar S. Karbonatlaşmanın Çelik Lifli ve Uçucu küllü Betonlarda Etkisi. Selcuk Univ J Eng, Sci & Technol/Selçuk Üniversitesi Mühendislik, Bilim ve Teknoloji Dergisi 2014;vol. 2.
[17] Okamura H, Tsuji Y, Maruyama K. Application of expansive concrete in structural elements. J Facul Eng B 1978;34.
[18] Nagataki S, Gomi H. Expansive admixtures (mainly ettringite). Cement Concr Compos 1998;20:163–70.
[19] Wang Y, Geng Y, Ranzi G, Zhang S. Time-dependent behaviour of expansive concrete-filled steel tubular columns. J Constr Steel Res 2011;67:471–83.
[20] Wang A, Deng M, Sun D, Mo L, Wang J, Tang M. Effect of combination of steel fiber and MgO-type expansive agent on properties of concrete. J Wuhan Univ Technol -Materials Sci Ed 2011;26:786–90.
[21] Wang L, Li G, Li X, Guo F, Tang S, Lu X, et al. Influence of reactivity and dosage of MgO expansive agent on shrinkage and crack resistance of face slab concrete. Cement Concr Compos 2022;126:104333.
[22] Mo KH, Alengaram UJ, Jumaat MZ, Yap SP, Lee SC. Green concrete partially comprised of farming waste residues: a review. J Clean Prod 2016;117:122–38.
[23] Nguyen HV, Nakarai K, Pham KH, Kajita S, Sagawa T. Effects of slag type and curing method on the performance of expansive concrete. Construct Build Mater 2020;262:120422.
[24] Shi Z, Lothenbach B. Role of aluminum and lithium in mitigating alkali-silica reaction—a. Horiz Mater 2022;8.
[25] Hay R, Ostertag CP. On utilization and mechanisms of waste aluminium in mitigating alkali-silica reaction (ASR) in concrete. J Clean Prod 2019;212:864–79.
[26] Chappex T, Scrivener KL. The influence of aluminium on the dissolution of amorphous silica and its relation to alkali silica reaction. Cement Concr Res 2012;42:1645–9.
[27] Linger D. Chemical expansion of fresh concrete by use of aluminum powder and its effect on strength. Highw Res Rec 1968.
[28] Jongprateep O, Jaroonvechatam N, Meesak T, Sujjavanich S. Effects of glass and limestone aggregates and aluminium on porosity, expansion, and strength of mortar bars. Mater Today Proc 2018;5:9306–11.
[29] Karalar M, Özkılıç YO, Deifalla AF, Aksoylu C, Arslan MH, Ahmad M, et al. Improvement in bending performance of reinforced concrete beams produced with waste lathe scraps. Sustain 2022;14:12660.
[30] Aksoylu C, Özkılıç YO, Hadzima-Nyarko M, Işık E, Arslan MH. Investigation on improvement in shear performance of reinforced-concrete beams produced with recycled steel wires from waste tires. Sustain 2022;14:13360.
[31] Batayneh M, Marie I, Asi I. Use of selected waste materials in concrete mixes. Waste Manag 2007;27:1870–6.
[32] Beskopylny A, Stel'makh SA, Shcherban EM, Mailyan LR, Meskhi B. Nano modifying additive micro silica influence on integral and differential characteristics of vibrocentrifuged concrete. J Build Eng 2022;51:104235.
[33] Kishore K, Gupta N. Application of domestic & industrial waste materials in concrete: a review. Mater Today Proc 2020;26:2926–31.
[34] Sandanayake M, Bouras Y, Haigh R, Vrcelj Z. Current sustainable trends of using waste materials in concrete—a decade review. Sustain 2020;12:9622.
[35] Sekar T, Ganesan N, Nampoothiri N. Studies on strength characteristics on utilization of waste materials as coarse aggregate in concrete. Int J Eng Sci Technol 2011;3:5436–40.
[36] Beskopylny AN, Shcherban' EM, Stel'makh SA, Meskhi B, Shilov AA, Varavka V, et al. Composition component influence on concrete properties with the additive of rubber tree seed shells. Appl Sci 2022;12:11744.
[37] Murali G, Vardhan CV, Prabu R, Khan ZMSA, Mohamed TA, Suresh T. Experimental investigation on fibre reinforced concrete using waste materials. Int J Eng Res Appl (IJERA) ISSN. 2012;2248:278–83.
[38] Kumar DP, Gladson GJN, Chandramauli A, Uma B, Sunagar P, Jeelani SH. Influence of reinforcing waste steel scraps on the strength of concrete. Mater Today Proc 2022;69.
[39] Zeybek Ö, Özkılıç YO, Karalar M, Çelik Aİ, Qaidi S, Ahmad J, et al. Influence of replacing cement with waste glass on mechanical properties of concrete. Materials 2022;15:7513.
[40] Basaran B, Kalkan I, Aksoylu C, Özkılıç YO, Sabri MMS. Effects of waste powder, fine and coarse marble aggregates on concrete compressive strength. Sustain 2022;14:14388.
[41] Çelik Aİ, Özkılıç YO, Zeybek Ö, Karalar M, Qaidi S, Ahmad J, et al. Mechanical behavior of crushed waste glass as replacement of aggregates. Materials 2022;15:8093.
[42] Karalar M, Bilir T, Çavuşlu M, Özkiliç YO, Sabri Sabri MM. Use of recycled coal bottom ash in reinforced concrete beams as replacement for aggregate. Front Mater 2022;9:1064604.
[43] Karalar M, Özkılıç YO, Aksoylu C, Sabri MMS, Alexey NB, Sergey AS, et al. Flexural behavior of reinforced concrete beams using waste marble powder towards application of sustainable concrete. Front Mater 2022:701.
[44] Qaidi S, Najm HM, Abed SM, Özkılıç YO, Al Dughaishi H, Alosta M, et al. Concrete containing waste glass as an environmentally friendly aggregate. A Rev Fresh Mech Charact 2022;15:6222.

[45] Fayed S, Madenci E, Onuralp Özkiliç Y, Mansour W. Improving bond performance of ribbed steel bars embedded in recycled aggregate concrete using steel mesh fabric confinement. Construct Build Mater 2023;369:130452.
[46] Sabapathy Y, Sabarish S, Nithish C, Ramasamy S, Krishna G. Experimental study on strength properties of aluminium fibre reinforced concrete. J Eng Sci King Saud Univ 2021;33:23–9.
[47] Çelik ES. Alüminyum döküm atık maddelerinin çevresel etkilerinin FMEA sistemi ile incelenmesi. 2007.
[48] Gödek E, Özdilli Ö, Kıvrak SO. Utilization of waste aluminum parts generated during CNC production as fiber in cement paste. International Conferences on Science and Technology Engineering Sciences and Technology ICONST EST 20202020.
[49] Muwashee RS, Al-Jameel HA, Jabal QA. Investigating the behavior of concrete and mortar reinforced with Aluminum waste strips. Int J Eng Technol 2018;7:211–3.
[50] Cabalar AF, Hayder G, Abdulnafaa MD, Isik H. Aluminum waste in road pavement subgrade. Ing Invest 2020;40:8–16.
[51] Kumar K, Dixit S, Arora R, Vatin NI, Singh J, Soloveva OV, et al. Comparative analysis of waste materials for their potential utilization in green concrete applications. Materials 2022;15:4180.
[52] Alfeehan A, Mohammed M, Jasim M, Fadehl U, Habeeb F. Utilizing industrial metal wastes in one-way ribbed reinforced concrete panels. Rev Ing Constr 2020;35:246–56.
[53] Małek M, Kadela M, Terpiłowski M, Szewczyk T, Łasica W, Muzolf P. Effect of metal lathe waste addition on the mechanical and thermal properties of concrete. Materials 2021;14:2760.
[54] Noori AQN, Aliewi JM, Salman HK, Numan HA. Investigation of lightweight structural materials produced using aluminum scraps with cement mortar. J Appl Eng Sci 2021;19:252–7.
[55] Mirza ZA, Khalid NN. Flexural behavior of reinforced lightweight concrete beams made with attapulgite and aluminum waste. J Eng Sustain Dev 2021;25:24–35.
[56] Zsutty TC. Shear strength prediction for separate categories of simple beam tests. ACI J 1971;68(2):138–43.